



## African Journal of Biological Sciences



# A Novel Robust CNN Model for MRI Brain Tumor Classification

Sulekha Das<sup>1</sup>, \*Dr. Avijit Kumar Chaudhuri<sup>2</sup>, Dr. Partha Ghosh<sup>3</sup>, Swagato Sikdar<sup>4</sup>

<sup>1</sup>Research Scholar, Information Technology, GCECT, Kolkata, West Bengal, India

<sup>2</sup>Associate Professor, Computer Science and Engineering, Brainware University, Barasat, West Bengal, India

<sup>3</sup>Assistant Professor, Computer Science and Engineering, GCECT, Kolkata, West Bengal, India

<sup>4</sup>Student –CSE-AIML(2nd year), Techno Engineering College Banipur

shu7773sea@gmail.com, c.avijit@gmail.com, parth\_ghos@rediffmail.com, sikdarswagato0@gmail.com

### Abstract

Brain tumors rank as the 10<sup>th</sup> leading cause of death for men and women, affecting both adults and children<sup>1</sup>. This underscores the urgent need for effective strategies in prevention, diagnosis, and treatment to address this significant health challenge. Magnetic resonance imaging (MRI) is the preferred method for identifying brain tumors. Recent advancements in image classification technology, particularly Convolutional Neural Networks (CNNs), have greatly improved tumor classification accuracy. The findings of this study have significant implications for clinicians specializing in the early detection of brain tumors. By leveraging advanced neural network models, healthcare professionals can potentially improve the accuracy and efficiency of tumor diagnosis, leading to better patient outcomes and possibly earlier interventions. This underscores the importance of leveraging cutting-edge technology, such as deep learning and neuroimaging, in medical diagnostics. In this study, CNNs are used for brain tumor classification, successfully categorizing brain images into two classes: benign and malignant with an impressive accuracy of 97%.

<sup>1</sup>[www.cancer.net](http://www.cancer.net)

**Keywords:** Convolutional Neural Network (CNN), Brain Tumor, Kappa score, Area Under the Curve (AUC)

Article History

Volume 6, Issue 5, 2024

Received: 15 May 2024

Accepted: 22 May 2024

doi:10.33472/AFJBS.6.5.2024.7113-7126

## Introduction

Brain tumors rank as the 10th leading cause of death for men and women, affecting both adults and children. This underscores the urgent need for effective strategies in prevention, diagnosis, and treatment to address this significant health challenge. Magnetic resonance imaging (MRI) is the preferred method for identifying brain tumors. Recent advancements in image classification technology, particularly the brain is, by far, the master organ of the human body, controlling the intricately intertwined processes of all other systems and making critical choices in our lives (Saba, 2020). Being the coordinator of the central nervous system, it controls both the voluntary activities and the involuntary processes that are a vital part of our body's functioning (Özyurt et al., 2020). While the heart serves as a critical organ that keeps us alive, the development of tumors within this vital structure poses considerable threats to our health and wellness.

Brain and central nervous system cancers represent a growing, frightful global public health challenge because of their high death rate, inflating costs to individuals and society, poor survival rate, and extremely low quality of life. As specified in the GLOBOCAN 2020 data, brain and central nervous system cancer is a significant share of the global causes of sickness (Ilic&Ilic, 2023). They are the 19th most frequent cancer, accounting for 1.9% of all cancers, and the 12th leading cause of cancer-related deaths, amounting to 2.5% of overall cancer deaths. Comprehensive, in-depth knowledge of the many aspects of brain tumors, like their symptoms, stage, and criticality, is very important for early diagnosis and solution. Magnetic Resonance Imaging (MRI) has been a base for clinicians to uncover internal subtle information about the brain structure and composition, including tumors (Sharif et al., 2021). Advanced computational methods, including deep learning, have demonstrated their capability to improve the accuracy and efficiency of tumor detection and classification.

On the contrary, it seems that a lot of articles have been written on this subject to summarize the current trends in DL, but they usually center around a very narrow part of the issue, which in the end leads to a situation in which we know too little about the field in its totality. Therefore, people do not have much idea about the scope of DL developments and how much they have grown up in this time.

In this regard, Convolutional Neural Networks (CNNs) have become an essential instrument for discerning and classifying different types of brain tumors, which include gliomas, meningiomas, pituitary tumors, and normal brain tissue. CNNs include multiple layers of interconnected neurons. When all of them are connected, they form a network that can learn complex patterns and features from data (Hu & Razmjoooy, 2021). Datasets with labeled brain images are the means of adjusting neurons' weights and biases across various layers for CNNs during the training process. Through repeated comparisons of predicted outputs and ground truth labels, the network refines its parameters to reduce errors and achieve the highest accuracy. This pattern of iterative learning occurs through the activation of functions, which introduces non-linearity and thus allows the network to capture internal relationships within the data.

The structure of CNNs is mainly the input layer, output layer, and at least one hidden layer is present. These layers act as key components in the feature extraction and abstraction processes, which enables the network to detect these sensitive distinctions. Moreover, trial and error with various parameters of the machine learning model like the number of layers, input filters, and learning rates positively impacts the diagnosis of different tissues (Mehnatkesh et al., 2023, Kumar & Mankame, 2020). Despite their computational complexity, CNNs deliver a unique function in dealing with and processing medical images and their capabilities to excel in the field of neuroimaging research cannot be devalued. Researchers constantly attempt to increase the efficacy of these deep learning models to enhance diagnostic precision, simplify clinical procedures, and finally, ensure the improvement of patient outcomes in the diagnosis and treatment of brain cancer.

### **Working of the proposed CNN model**

The architecture of the experimental layout of this research and model construction is presented in Fig.1. A CNN in PyTorch is formulated from constituent layers which include convolutional, pooling, and fully connected layers, to build the model structure. These levels are necessary to build up hierarchical representations of features from input data consideration, especially for tasks like image classification. The process consists of creating an initial Python class consisting of the CNN model. All these layers are set as an initial layer where parameters are defined, such as the kernel size, the number of filters, and activation functions. For instance, the authors start with four convolution layers followed by pooling layers to down sample the feature map and simply connected layers for classification. After the creation of these layers, they are passed into the forward function of the class one

by one, which produces the outputs of the specific network. It is a key part of the network where data undergoes convolutional operations, followed by pooling, and then steps through fully connected layers ultimately. With this connected architecture, information flows in a predefined order during both prediction and training (backward pass) to facilitate the efficient propagation of information through the network.

The model is trained with image datasets after constructing architecture. This is done by feeding the input images through the network one after another, computing loss between predicted and actual labels, and then using techniques like backpropagation and optimization algorithms (like Stochastic Gradient Descent, Adam) to update network parameters iteratively. There is an automatic learning functionality enabled that allows the convolutional and pooling layers to learn effective feature representations from the input images. This is done through the process of optimization of parameters. One of the biggest strengths of CNNs is their ability to learn detailed features directly from data making them suitable for achieving outstanding performance across several computer vision tasks.

The authors employed several strategies to enhance the performance of their Convolutional Neural Network (CNN) model for vision tasks:

**Adding More Layers:** Through an increase in the depth of the CNN architecture, the model is essentially capable of learning more complex elements and features from the input data. This leads to the acquisition of better precision and increases the overall quality of the model.

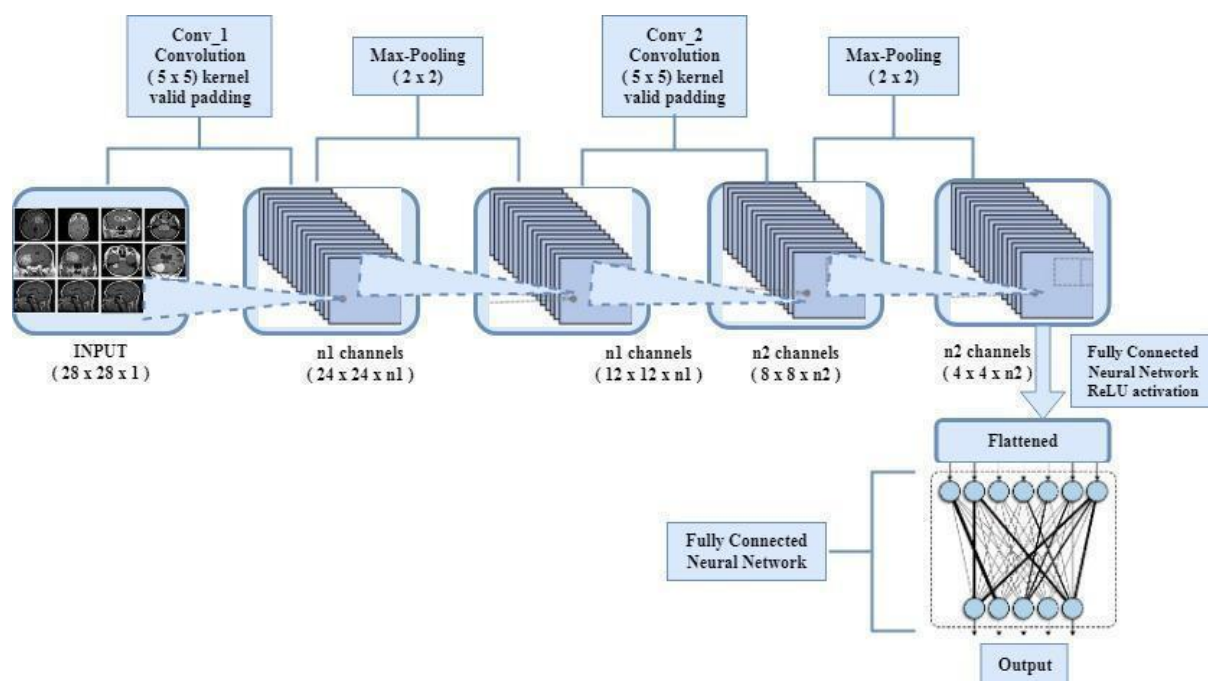
**Training for More Epochs:** A rise of epochs means that the model will see the training data more times, which helps higher convergence to fine-tuned features. Thus, the model can create more complex embeddings that manage to encapsulate a greater diversity of features that can be found in the input data.

**Fine-tuning Hyperparameters:** Hyperparameters like learning rate and regularization strength are very important in the training process. Through the selection of grid search or random search methods, the authors aim to find the exact setting of all hyperparameters that will guarantee the perfect model to run. The adjustment of the learning rate determines the step size during parameter update and thus affects the speed and stability of training. Regularization techniques act as a buffer against overfitting in complex models by imposing penalties.

**Experimentation and Iterative Improvement:** The authors use the cycle of trial and error to improve the model by iteratively adjusting the model architecture, training procedures, and parameters depending on the feedback. Therefore, this process involves systematically exploring different configuration options and strategies to find the best-performing model to match the specific vision tasks.

The authors will implement these strategies and will never cease refining their model through experimentation to achieve the accuracy and robustness of the vision tasks given. Therefore, this iterative process shows that a model should meet high initial standards and also be improved and optimized during the whole learning process. The architecture for the proposed classifier for brain cancer prediction has been depicted in Figure 1 below.

Figure 1: Brain Cancer Prediction Framework



## Relevant Literature

According to McCaley(2015), knowledge classification (normal vs. mutated brains) should prevail, and brain tumors have to be predicted more carefully. Within the scope of research, the researchers employ a wide range of machine learning techniques, which consist of a Support Vector Machine (SVM), K-nearest neighbor (KNN), and Hybrid Classifier (SVM-KNN). Through the use of such tools, they classified the 50-image dataset. Data show that the SVM-KNN classifier method has a top accuracy level of 98% when compared to the rest of the trained methods. This paper's main aim is to show the improvement in MRI brain cancer classification accuracy, especially with the SVM-KNN hybrid classifier application.

Afshar et al., 2018 indicate, that the early and precise diagnosis of brain tumors is complicated based on brain tumors' different severity and incidence across different age groups. Convolution neural networks (CNNs) are suitable for this type of task, but they require trained data and also cannot handle input transformations. Capsule Network (CapsNets), the breakthrough in machine learning architectures, is a natural choice here since it is more robust to transformations and requires a smaller training set, which makes it perfect for such a small dataset and brain MRI images.

Experimental data show that CapsNet has a CNN (convolutional neural network) structure, performing better than the others in the deep learning area, including imaging tasks, especially in the field of medicine.

Zacharaki et al., 2019, focused on pattern classification methods capable of recognizing cluster differences, for example, between primary gliomas and brain metastases, and glioma grading. They invented unique methods of classification that are capable of integrating conventional MRI and perfusion MRI for better differentiation ability. The methodology consists of a series of steps such as region of interest (ROI) definition, feature extraction, feature selection, and classification. The extended characteristics in principle include the shape and intensity data and the rotation-invariant texture features. A feature subset is a result of using a support vector machine algorithm with recursive feature elimination.

Sajjad et al., 2019 proposed a novel multi-grade classification system for brain tumor diagnosis based on the CNN approach, which aims to alleviate the work burden of radiologists and better utilize MRI data. The suggested system is verified through data augmentation and the original data. It shows a better performance than existing ones. The results have demonstrated the efficiency of this method in accurate and reliable brain tumor classification. Thus, radiologists can work properly based on medical imaging analysis.

Deepak et al., 2019 present a new approach to brain tumor classification in which three different types of tumors are identified: Glioma, meningioma, and pituitary are the major three diseases to be detected by the deep convolutional transfer learning approach. The methodology includes the use of the GoogLeNet model that has been pre-trained to produce the image attributes from the MRI images of the brain. Subsequently, these features shall be given to trained classifier models so that classification can be performed. This study randomly applies a patient-level, five-fold cross-validation process to MRI data collected through Figshare. The obtained results reveal a highly accurate mean classification accuracy of 98%. Performance metrics, e.g., AUC, Precision, Recall, F-score, and Specificity are also

computed. On the other hand, this paper reveals the practicality of small training samples, based on transfer learning, which is shown in this case. The outcomes prove that deep transfer learning is an effective method in medical image analysis, especially when the data is less available.

Deb et al.(2024) in their proposed work, make use of deep neural network form, which is a type of convolutional neural network (CNN) to classify images into TUMOUR DETECTED and TUMOUR NOT DETECTED. The model has achieved outstanding results in terms of accuracy, with a mean accuracy score of 96.08% and a fscore of 97.3. This suggests that such models can detect tumors precisely in MRIs and hence demonstrate the path with deep learning methods used in the field of medical image analysis and diagnosis.

Ayadi et al., 2021 noted that the main aim of brain tumors classification results from their grave consequences as well as different classifications. Moreover, the new CNN-based model, which can differentiate between brain tumors in MRI images, is illustrated in the first instance. This model has been made up of numerous layers of the network to achieve decent classification accuracy for brain tumors.

Table 1. Summary of recent work that has been performed in brain cancer detection and in this research using machine learning and deep learning algorithms

| <b>Author</b>         | <b>Feature/methods</b>         | <b>Performance(%)</b>   |
|-----------------------|--------------------------------|---|
| Sasikala et al., 2008 | DWT, GA, ANN                   | Accuracy = 98<br>Sensitivity = NA<br>Specificity = NA<br>AUC = NA       |
| Verma et al., 2008    | Bayesian, and SVM              | Accuracy = NA<br>Sensitivity = 91.84<br>Specificity = 99.57<br>AUC = NA |
| Zacharaki et al.,     | SVM, RFE Feature Ranking, LDA, | Accuracy = 97.8   |

|                       |  |   |
|-----------------------|--|---|
| 2009                  | KNN, NL-SVM  | Sensitivity = 100<br>Specificity = 95<br>AUC = 98.6                     |
| Ryu et al., 2014      | GLCM, Entropy, Histogram   | Accuracy = 84.4<br>Sensitivity = 81.8<br>Specificity = 90<br>AUC = 94.1 |
| Machhale et al., 2015 | SVM-KNN  | Sensitivity = 100<br>Specificity = 93.75<br>Accuracy = 98               |
| Cheng et al., 2015    | Feature extraction: Intensity, histogram, GLCM, BOW, classification Methods: SVM, SRC, KNN | Accuracy = 91.28  |
| Skogenet al., 2016    | Statistical Analysis and Standard Deviation  | Accuracy = 84.4<br>Sensitivity = 93<br>SPC = 81<br>AUC = 91             |
| Paul et al., 2017     | CNN  | Accuracy = 84.19  |
| Afshar et al., 2018   | Capsule network method   | Accuracy = 86.56  |
| Zia et al., 2018      | Window based image cropping  | Accuracy = 85.69<br>Sensitivity = 86.26<br>Specificity = 90.90          |



|                               |  |  |
|-------------------------------|--|--|
| Sajjad et al., 2019           | CNN with data augmentation   | Accuracy = 94.58<br>Sensitivity = 88.41<br>Specificity = 96.12                             |
| Badža&Barjaktarovi<br>c, 2020 | CNN  | Accuracy = 95.40   |
| Huang et al., 2020            | Convolutional Neural Network Based<br>on Complex Networks (CNNBCN) | Accuracy = 95.49   |
| This Study                    | CNN  | Accuracy = 97<br>Sensitivity = 96<br>Specificity = 98<br>Kappa Score = 94<br>AUC/ ROC = 97 |

## Methodology

### Dataset Description

The dataset used in this study for the brain tumor classification was acquired from Kaggle, containing around 3762 MRI images. The dataset contains 2079 images without any tumors and 1683 images with tumors. These images, which are segmented into training and testing, are used for the creation of models. The training data corresponds to the part of input information used for the learning process, whereas the testing data is used to test performance. The dataset has been divided into training and testing groups in various ratios, such as 60/40, 70/30 and 80/20 train/test partitions, and 10-fold cross-validation. In cross-validation, the dataset is split into mutually exclusive subsets, and the training and testing are done through the different subset combinations. To illustrate this, **Figure #** demonstrates some data that will be used for experimental purposes. The visualization part of the process can, therefore, be of help in understanding the general qualities and features of the dataset that is being examined.

**Convolutional Neural network:**

A Convolutional Neural Network (CNN) is an exemplary deep learning architecture that was developed for dealing with structured grid data frameworks such as images. The structure consists of several layers, wherein each layer performs specific functions and is stacked in hierarchical order to extract the salient features from the input data.

**Input Layer:** The input layer receives the raw image data, typically represented as a matrix of pixel values.

**Convolutional Layer:** A Convolutional Neural Network (CNN) is a typical deep learning architecture that was created specifically to solve the problems of data with grid structures, e.g. images. The structure is made up of a sequence of layers. Each layer has its own function to accomplish, and each layer has a hierarchical order trying to extract the salient features of the input data.

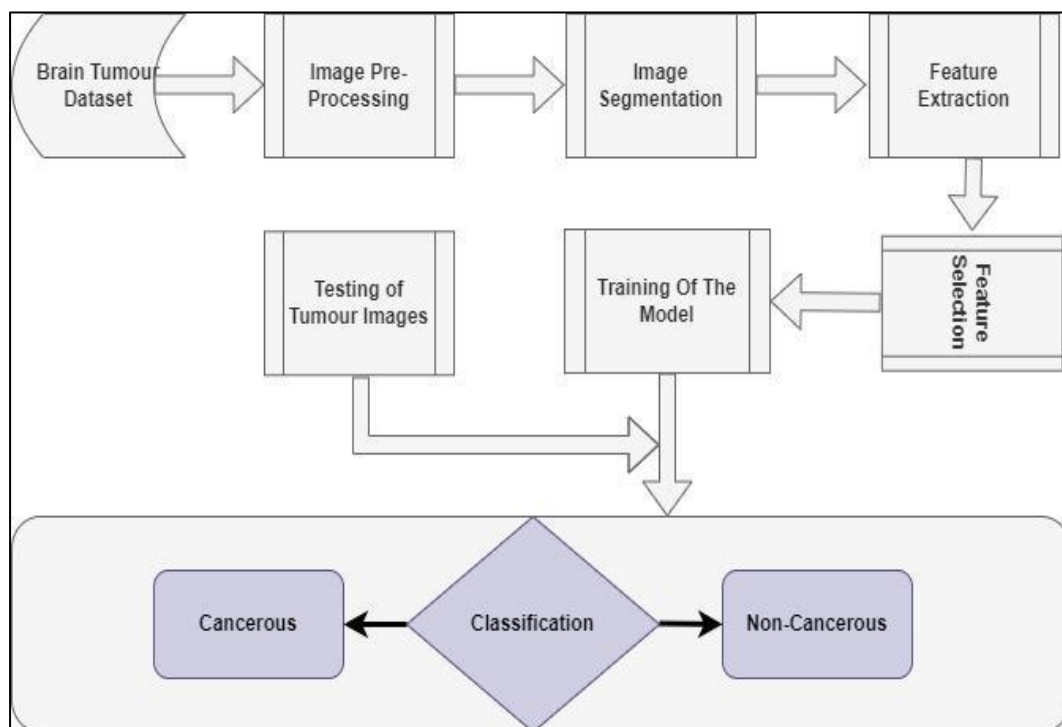
**Pooling Layer:** The pooling layer manages the spatial dimensions of the feature maps obtained from the convolutional layers by downsizing. Max pooling, a widely used method, picks the maximum from each of the local areas (e.g., 2x2) of the feature map. One of the roles of Max pooling is to reduce computational complexity, make the network more tolerant of minor input differences, and minimize over-fitting. In addition, pooling layers capture the most important features and dispose of unrelated information while minimizing sensitivity to the input translations.

**Fully Connected (FC) Layer:** The fully connected layers integrate the detected features by the convolutional and pooling layers for the purpose of classification or regression. Every single neuron in a fully connected layer is connected to every neuron in the previous layer, so it forms a tightly packed structure. Unlike CNN, FC layers focus on learning the interrelationships between features and making the final predictions. We may use activation functions such as Softmax to assign class probabilities from the fully connected layer output.

**Output Layer:** The output layer generates the final predicted or classified results. For the classification tasks, it mainly uses the softmax activation function to convert raw scores into the degree of probability of belonging to classes. The network's output shows the confidence interval for the output classes.

**Feature Map:** Feature maps, as the output of convolutional layers, encode learned features. They referred to as convolutional neural network (CNN) is structured grids of activation values, where each value represents either the existence or the lack of a specific feature at a given position in the input. Feature maps are partitioned into the overlapped sets to perform pooling operations, which are considered as the most important information either with the max pooling or the average pooling. In summary, CNNs make use of convolutional and pooling operations to extract hierarchical features from input images and finally fully connected layers to make decisions based on these features. This architecture obtained remarkable result in numerous computer vision tasks, such as image classification, object detection, and segmentation. (Ting et al., 2019; Dang et al., 2019). Figure 2 demonstrate the CNN architecture.

Figure 2. CNN architecture for brain tumor diagnosis



### CNN in Cancer Research

CNNs have been of interest to many researchers in their ability to process and analyze images as well as recognize patterns. Here are some key reasons why CNNs are extensively used in cancer research:

**Feature Extraction from Medical Images:**

CNNs can learn hierarchical image representations automatically and consequently can extract intricate features from MRI and CT images as a result. These features are particularly important in detecting even small abnormalities suggestive of cancer(Litjens et al., 2017).

**Classification and Diagnosis:**

CNNs are capable of classifying medical images as belonging to various categories that in turn may be utilized for different cancer diagnoses. They are trained to learn discriminative features and then are able to give a precise classification of the available data to the healthcare professionals for informative decisions(Esteva et al., 2017).

**Segmentation of Tumor Regions:**

The CNNs can segment tumour regions in medical images highlighting the edges of cancerous tissues. Precise segmentation is vital for treatment planning, monitoring disease progression and checking the effectiveness of treatment(Litjens et al., 2016)..

**Prediction of Treatment Response:**

CNNs can forecast the response of tumors to specific treatment with help of pre-treatment imaging data. Through the analysis of tumor characteristics change, CNNs play role in tailoring treatments to specific patients to achieve better outcomes(Parmar et al., 2017).

**Prognostication and Survival Prediction:**

CNNs can analyze medical images to extract prognostic biomarkers indicative of patient outcomes. By identifying imaging features associated with disease aggressiveness, CNNs can aid in predicting patient survival and stratifying risk(Wulczyn et al., 2020).

The extensive integration of CNNs in cancer research spanning diverse applications, highlighting their capacity to transform cancer diagnosis, treatment, and prognosis forecasting.

**Results and Discussion**

A comprehensive breakdown of various performance metrics commonly used in binary classification problems is described below.

**Accuracy:** Accuracy can measure the overall correctness of the classifier. It records the ratio of correctly classified instances (both positive and negative) that are classified correctly to the total number of instances, as depicted in the equation (1)

$$\text{Accuracy} = \frac{\text{TP} + \text{TN}}{\text{FP} + \text{FN} + \text{TP} + \text{TN}} \quad (1)$$

**Sensitivity(Recall):** Sensitivity, which for most cases is known as predictive value or true positive rate, is defined as the probability of getting the correct disease class and it is depicted in the formula (2).

$$\text{Sensitivity} = \frac{\text{TP}}{\text{FN} + \text{TP}} \quad (2)$$

**Specificity:** Specificity is defined as the proportion of actual true negative cases that are classified as negative by the method. It is depicted as shown in the formula (3).

$$\text{Specificity} = \frac{\text{TN}}{\text{FP} + \text{TN}} \quad (3)$$

**Precision:** The measures of precision are the number of instances of positive test results correctly diagnosed over all the positive tests. It is shown in the formula (4).

$$\text{Precision} = \frac{\text{TP}}{\text{FP} + \text{TP}} \quad (4)$$

**False Positive Rate (FPR):** The FPR is a ratio of the proportion of true negative to that of the corresponding false positive and represented by the mathematical function (5).

$$\text{FPR} = \frac{\text{FP}}{\text{TN} + \text{FP}} \quad (5)$$

**F1 Score:** F1 score is the harmonic mean (HM) of precision and recall rates. It gives a balance between precision and recall, and used when classes are imbalanced. It is represented by the mathematical function (6).

$$\text{F1Score} = \frac{2 \times \text{Recall} \times \text{Precision}}{\text{Recall} + \text{Precision}} \quad (6)$$

$$\text{AUC} = \frac{1}{2}(1 + \text{Sensitivity} - \text{FPR}) \quad (7)$$

$$\text{Kappa Statistic} = \frac{2 \times (\text{TP} \times \text{TN} - \text{FN} \times \text{FP})}{(\text{TP} \times \text{FN} + \text{TP} \times \text{FP} + 2 \times \text{TP} \times \text{TN} + \text{FN}^2 + \text{FN} \times \text{TN} + \text{FP}^2 + \text{FP} \times \text{TN})} \quad (8)$$

The accuracy, recall, specificity, Kappa statistics and AUCs are the basis of comparison and are depicted in Tables 2-5, respectively.

Table 2. Comparison of accuracies for train/ test partitions(Epoch 30)

| <b>Train/<br/>Partitions</b> | <b>Test</b> | <b>Accuracy<br/>Metrics</b> | <b>Tumours<br/>Prediction<br/>Accuracy()</b> |
|------------------------------|-------------|-----------------------------|--|
| <b>60-40</b>                 |             | Accuracy                    | 92.35  |
|                              |             | Sensitivity                 | 92   |
|                              |             | Specificity                 | 93   |
|                              |             | AUC                         | 92   |
|                              |             | Kappa Score                 | 84   |
| <b>70-30</b>                 |             | Accuracy                    | 92   |
|                              |             | Sensitivity                 | 91   |
|                              |             | Specificity                 | 92   |
|                              |             | AUC                         | 91   |
|                              |             | Kappa Score                 | 83   |
| <b>80-20</b>                 |             | Accuracy                    | 91   |
|                              |             | Sensitivity                 | 86   |
|                              |             | Specificity                 | 95   |
|                              |             | AUC                         | 90   |

|  |             |    |
|--|-------------|----|
|  | Kappa Score | 80 |
|--|-------------|----|

Table 3. Comparison of accuracies for 10 fold cross validations(Epoch 30)

| <b>Train/ Test Partitions</b> | <b>Accuracy Metrics</b> | <b>Tumours Prediction Accuracy()</b> |
|-------------------------------|-------------------------|--------------------------------------|
| <b>1st fold</b>               | Accuracy                | 91                                   |
|                               | Sensitivity             | 82                                   |
|                               | Specificity             | 97                                   |
|                               | AUC                     | 97                                   |
|                               | Kappa Score             | 80                                   |
| <b>2nd fold</b>               | Accuracy                | 92                                   |
|                               | Sensitivity             | 86                                   |
|                               | Specificity             | 97                                   |
|                               | AUC                     | 90                                   |
|                               | Kappa Score             | 83                                   |
| <b>3rd fold</b>               | Accuracy                | 94                                   |
|                               | Sensitivity             | 92                                   |
|                               | Specificity             | 95                                   |
|                               | AUC                     | 95                                   |
|                               | Kappa Score             | 87                                   |
| <b>4th</b>                    | Accuracy                | 94.5                                 |
|                               | Sensitivity             | 92.34                                |
|                               | Specificity             | 96.22                                |

|            |             |       |
|------------|-------------|-------|
|            | AUC         | 94    |
|            | Kappa Score | 88.3  |
| <b>5th</b> | Accuracy    | 93.45 |
|            | Sensitivity | 93    |
|            | Specificity | 95    |
|            | AUC         | 92    |
|            | Kappa Score | 87    |
| <b>6th</b> | Accuracy    | 93    |
|            | Sensitivity | 87    |
|            | Specificity | 96    |
|            | AUC         | 92    |
|            | Kappa Score | 85    |
| <b>7th</b> | Accuracy    | 92.38 |
|            | Sensitivity | 89    |
|            | Specificity | 95.4  |
|            | AUC         | 94    |
|            | Kappa Score | 85    |
| <b>8th</b> | Accuracy    | 94    |
|            | Sensitivity | 91    |
|            | Specificity | 96    |
|            | AUC         | 93    |
|            | Kappa Score | 87    |
| <b>9th</b> | Accuracy    | 91    |



|             |             |    |
|-------------|-------------|----|
|             | Sensitivity | 87 |
|             | Specificity | 94 |
|             | AUC         | 94 |
|             | Kappa Score | 81 |
| <b>10th</b> | Accuracy    | 97 |
|             | Sensitivity | 96 |
|             | Specificity | 98 |
|             | AUC         | 93 |
|             | Kappa Score | 94 |

This research provides insight into how MRI technology plays a crucial role in detecting brain tumors, with the main focus being to interpret MRI images using deep learning algorithms and detect cancer cells. The authors aimed to integrate these algorithms into medical practice and in particular use data from open sources and multiple medical centres.

The authors used a CNN to successfully achieve their goals which they implemented using the PyTorch machine learning library and coded in Python. We split the data into the 10 fold cross validation and various train-test splits (60-40, 70-30, and 80-20) and retrained the model for the 30 epochs, with batch size 32 for every epoch.

The results were promising and the model illustrated considerable accuracy rates, especially 97% accuracy (as shown in Table 3) for the final epoch with 10-fold cross-validation. This accuracy was also similar irrespective of the train-test splits. Moreover, the model manifested excellent sensitivity, specificity, and kappa scores, approximately 96%, 98%, and 94% respectively, particularly for the discrimination between benign and malignant nodes. These performance metrics still remain stable despite the variation of data splits.

Table 4. Comparison of AUCs(train/test partition) for30 epochs

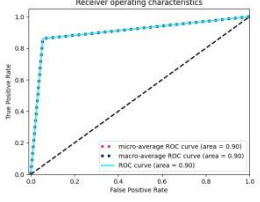
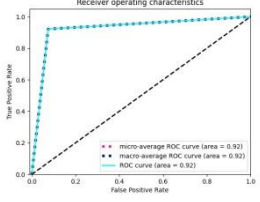
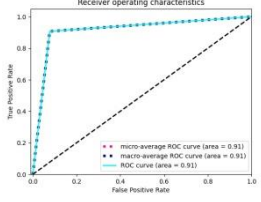
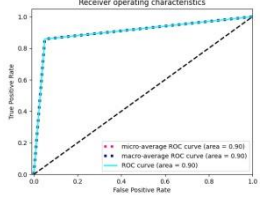
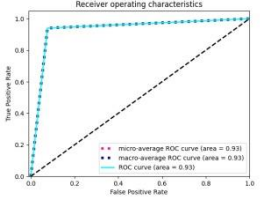
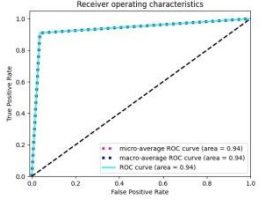
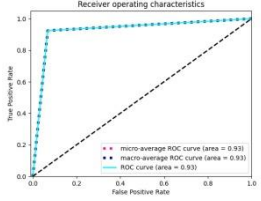
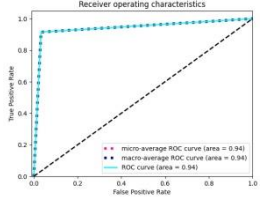
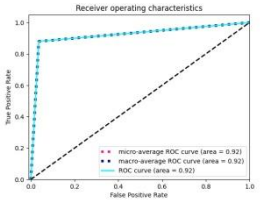
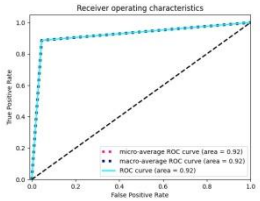
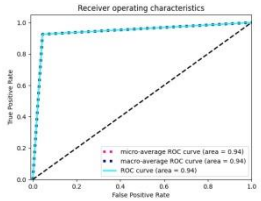
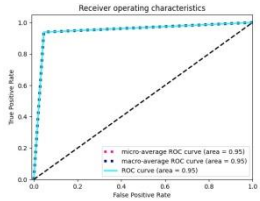
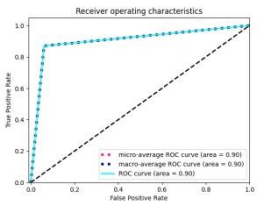
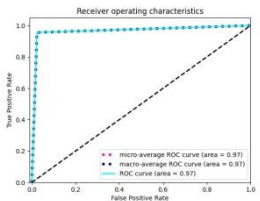
|   |   |  |   |
|---|---|--|---|
|  <p>Receiver operating characteristics</p> <ul style="list-style-type: none"> <li>micro-average ROC curve (area = 0.90)</li> <li>macro-average ROC curve (area = 0.90)</li> <li>ROC curve (area = 0.90)</li> </ul> |  <p>Receiver operating characteristics</p> <ul style="list-style-type: none"> <li>micro-average ROC curve (area = 0.92)</li> <li>macro-average ROC curve (area = 0.92)</li> <li>ROC curve (area = 0.92)</li> </ul> |  <p>Receiver operating characteristics</p> <ul style="list-style-type: none"> <li>micro-average ROC curve (area = 0.93)</li> <li>macro-average ROC curve (area = 0.93)</li> <li>ROC curve (area = 0.93)</li> </ul> |  <p>Receiver operating characteristics</p> <ul style="list-style-type: none"> <li>micro-average ROC curve (area = 0.90)</li> <li>macro-average ROC curve (area = 0.90)</li> <li>ROC curve (area = 0.90)</li> </ul> |
| 50/50   | 60/40   | 70/30  | 80/20   |

Table 5. Comparison of AUCs(10 fold cross validation) for 30 epochs

|   |   |  |   |
|---|---|--|---|
|  <p>Receiver operating characteristics</p> <ul style="list-style-type: none"> <li>micro-average ROC curve (area = 0.93)</li> <li>macro-average ROC curve (area = 0.93)</li> <li>ROC curve (area = 0.93)</li> </ul>   |  <p>Receiver operating characteristics</p> <ul style="list-style-type: none"> <li>micro-average ROC curve (area = 0.94)</li> <li>macro-average ROC curve (area = 0.94)</li> <li>ROC curve (area = 0.94)</li> </ul>   |  <p>Receiver operating characteristics</p> <ul style="list-style-type: none"> <li>micro-average ROC curve (area = 0.93)</li> <li>macro-average ROC curve (area = 0.93)</li> <li>ROC curve (area = 0.93)</li> </ul>   |  <p>Receiver operating characteristics</p> <ul style="list-style-type: none"> <li>micro-average ROC curve (area = 0.94)</li> <li>macro-average ROC curve (area = 0.94)</li> <li>ROC curve (area = 0.94)</li> </ul>   |
| 10 th fold  | 9 th fold   | 8 th fold  | 7th fold  |
|  <p>Receiver operating characteristics</p> <ul style="list-style-type: none"> <li>micro-average ROC curve (area = 0.92)</li> <li>macro-average ROC curve (area = 0.92)</li> <li>ROC curve (area = 0.92)</li> </ul> |  <p>Receiver operating characteristics</p> <ul style="list-style-type: none"> <li>micro-average ROC curve (area = 0.92)</li> <li>macro-average ROC curve (area = 0.92)</li> <li>ROC curve (area = 0.92)</li> </ul> |  <p>Receiver operating characteristics</p> <ul style="list-style-type: none"> <li>micro-average ROC curve (area = 0.94)</li> <li>macro-average ROC curve (area = 0.94)</li> <li>ROC curve (area = 0.94)</li> </ul> |  <p>Receiver operating characteristics</p> <ul style="list-style-type: none"> <li>micro-average ROC curve (area = 0.93)</li> <li>macro-average ROC curve (area = 0.93)</li> <li>ROC curve (area = 0.93)</li> </ul> |
| 6th fold  | 5 th fold   | 4th fold   | 3rd fold  |
|  <p>Receiver operating characteristics</p> <ul style="list-style-type: none"> <li>micro-average ROC curve (area = 0.90)</li> <li>macro-average ROC curve (area = 0.90)</li> <li>ROC curve (area = 0.90)</li> </ul> |  <p>Receiver operating characteristics</p> <ul style="list-style-type: none"> <li>micro-average ROC curve (area = 0.97)</li> <li>macro-average ROC curve (area = 0.97)</li> <li>ROC curve (area = 0.97)</li> </ul> |  |   |
| 2nd fold  | 1st fold  |  |   |

The ROCs(Receiver Operating Characteristic) shown in Table 5 represent the performance metrics of the designed CNN model in this experiment using a 10-fold cross-validation techniques and train/ test partitions. ROC charts are among the most widely used graphical methods to evaluate binary classifiers. The receiver operating characteristic curve shows the tradeoffs between true positive rate and false positive rate. The experiment proves that the proposed classifier, developed by the authors in the said study, was better performing compared to most of the models discussed in the literature review. The proposed classifier showed outstanding performance when the AUC/ROC values were being evaluated using 10 fold cross validations and several train/ test partitions. The AUC value achieved by the proposed model was 0.97, which is the highest possible value, illustrating great distinction ability between the two classes. Hence this new CNN model seems to be very helpful in distinguishing between the classes. High ROC values indicate the strong predictive ability of model that can have practical implications in real world applications in the binary classification problems.

One of the interesting findings of the research was the recognition of difficult cases where benign nodules looked like malignant ones. In addition to these difficulties, the algorithm proved to be quite robust in assignments, displaying its capabilities to recognize benign and malignant nodules even in visually unclear cases.

Table 6. Accuracies for 80/ 20 train/ test partitions with reduced convolutional and max-pooling layers

| <b>Train/ Test Partitions</b> | <b>Accuracy Metrics</b> | <b>Tumors Prediction Accuracy</b> |
|-------------------------------|-------------------------|-----------------------------------|
| <b>80-20</b>                  | Sensitivity             | 32                                |
|                               | Specificity             | 07                                |

Using Explainable Artificial Intelligence (XAI), we could explain the changes in model performance that are observed when convolutional layers and max-pooling layers are reduced by 1 as illustrated in Table 6. These techniques enable one to see the impact of changes in the architecture of the model on different aspects of performance.

Here's a breakdown of the observed changes and potential explanations using XAI principles:

### 1. Recall for Malignancy Class Drop (0.86 to 0.32):

- **Class-Specific Sensitivity:** Recall evaluates the capacity of the model to identify the positive samples of a certain class, in this case, the malignant instances.

**Explanation:** The marked reduction in the recall shows that the proposed model with fewer convolutional and max-pooling layers is not as successful in identifying malignant instances. This is likely because:

**Insufficient Feature Learning:** However, this may lead to the fact that the model does not learn rich or deep features that would help to distinguish between malignant cases and others.

**Loss of Fine-Grained Details:** As one can gather, the model might neglect important patterns necessary for classifying malignant cases due to the simplification of the network architecture.

**Class Imbalance Handling:** If malignant cases are less frequent, decreasing model capacity could bias the model for this class, which ultimately leads to a higher number of missed malignant cases.

### 2. Specificity for Malignancy Prediction Drop (0.95 to 0.07):

- **False Positives Increase:** Specificity evaluates the model in correctly identifying negative cases, which is a non-malignant instance.

**Explanation:** The dramatic reduction in specificity means that the model misidentifies a large number of benign or normal cases as malignant. This could be due to:

**Lack of Feature Distinction:** Such reduction may not help in making a correct distinction between malignant and non-malignant cases due to poor feature extraction.

**Overgeneralization:** If there were fewer layers, then the model would become too general and may classify even benign cases as malignant.

**Feature Overlap:** It is possible that there are features that can assist in discriminating malignancy that are not well learned or represented in the model, thus misclassifying benign cases as malignant ones.

In general, this research reveals the ability of deep learning algorithms integrated into MRI technology to correctly diagnose and classify brain cancer as a good instrument for medical professionals in diagnosis and treatment planning.

### **Conclusion:**

This paper demonstrates how transfer learning, especially the use of a deep convolutional neural network (CNN), can help with the precise diagnosis of different types of brain cancer through magnetic resonance imaging (MRI) scans. The model shown in the given paper uses sigmoid and ReLU activation functions and successfully gets an outstanding score on every evaluation metric that can be used to measure accuracy. Moreover, this shows how powerful the model is in correctly classifying the images into their proper classes. The highest accuracy that was achieved here manifests the model's success in amplifying early diagnosis and customizing treatment plans for brain cancer patients for clinicians. Such screening is expected to bring many benefits to the process, starting with the quick and precise recognition of different types of tumors from MRI scans. This method has the prospect of optimizing therapeutic outcomes and contributing to early detection that might ultimately result in improved patient prognosis.

Bringing together several performance metrics like accuracy, sensitivity, specificity, kappa and AUC (Area Under the ROC Curve) while analyzing brain cancer models is a significant advance in the field of model evaluation. Normally, researchers usually pay attention to only one or two metrics that typically comprise of accuracy. On the other hand, such a step might leave out several other aspects of model performance, including a situation where different metrics demonstrate various facets of the model's behaviour, especially in medical applications.

Through the employment of all these metrics, our CNN model of brain cancer detection offers a holistic assessment of its performance. Achieving the best accuracy across all the metrics demonstrates our model's capability to excel in different modes of evaluation. This integrational strategy is not only the evidence of model distinction but also the proof of feasibility of such concept in practical health-care domain.

Finally, the use of advanced deep learning techniques in medical image analysis as presented in the research indicates the likelihood of the development of early diagnosis and better living of patients in the context of oncology, especially in the case of brain cancer. This advanced approach shows us how to harness the potential of artificial intelligence to improve health systems and thus patients' well-being.

### **Future Scope**

The actual accuracy score of around 98% by the developed model with the help of all performance metrics suggests best possibilities for future applications in the field of medical image analysis. The efficacy of this model demonstrates its potential is not limited to other disease datasets. Instead, it shows the way to the early identification and classification of numerous other medical conditions.

In the upcoming period, the extent of this research can be augmented by working jointly with healthcare agencies and hospitals to collect varied datasets. Researching different ways to do the tasks, including applying reinforcement learning methods, can help to raise the level of model performance. These may entail tweaking the current model architecture, implementing new neural network machines, or application of advanced algorithms for the best outcomes.

Furthermore, this model can be developed for present-day diagnosis and treatment monitoring, which helps in the creation of more personalized and timely interventions. The integration of artificial intelligence into healthcare is a rapidly growing field, and the success illustrated in this study gives the basis for further innovation and testing of various solutions to enhance early disease diagnosis and improve patients' outcomes.

**Data Availability Statement (DAS):** The dataset used in this study for the brain tumor classification was acquired from kaggle.com and this does not violate the protection of human subjects, or other valid ethical, privacy, or security concerns

**Data Availability Statement (DAS):** The dataset used in this study for the brain tumor classification was acquired from kaggle.com and this does not violate the protection of human subjects, or other valid ethical, privacy, or security concerns

### **References**

Afshar, P., Mohammadi, A., & Plataniotis, K. N. (2018, October). Brain tumor type classification via capsule networks. In 2018 25th IEEE international conference on image processing (ICIP) (pp. 3129-3133). IEEE.

- Ayadi, W., Elhamzi, W., Charfi, I., & Atri, M. (2021). Deep CNN for brain tumor classification. *Neural processing letters*, 53, 671-700.
- Badža, M. M., & Barjaktarović, M. Č. (2020). Classification of brain tumors from MRI images using a convolutional neural network. *Applied Sciences*, 10(6), 1999.
- Cheng, J., Huang, W., Cao, S., Yang, R., Yang, W., Yun, Z., ... & Feng, Q. (2015). Enhanced performance of brain tumor classification via tumor region augmentation and partition. *PloS one*, 10(10), e0140381.
- Dang, L. M., Hassan, S. I., Im, S., & Moon, H. (2019). Face image manipulation detection based on a convolutional neural network. *Expert Systems with Applications*, 129, 156-168.
- Deb, D., Khang, A., & Chaudhuri, A. K. (2024). Fuzzy Thresholding-Based Brain Image Segmentation Using Multi-Threshold Level Set Model. In *Driving Smart Medical Diagnosis Through AI-Powered Technologies and Applications* (pp. 118-129). IGI Global.
- Deepak, S., & Ameer, P. M. (2019). Brain tumor classification using deep CNN features via transfer learning. *Computers in biology and medicine*, 111, 103345.
- Esteva, A., Kuprel, B., Novoa, R. A., Ko, J., Swetter, S. M., Blau, H. M., & Thrun, S. (2017). Dermatologist-level classification of skin cancer with deep neural networks. *nature*, 542(7639), 115-118.
- Hu, A., & Razmjoooy, N. (2021). Brain tumor diagnosis based on metaheuristics and deep learning. *International Journal of Imaging Systems and Technology*, 31(2), 657-669.
- Huang, Z., Du, X., Chen, L., Li, Y., Liu, M., Chou, Y., & Jin, L. (2020). Convolutional neural network based on complex networks for brain tumor image classification with a modified activation function. *IEEE Access*, 8, 89281-89290.

- Ilic, I., &Ilic, M. (2023). International patterns and trends in the brain cancer incidence and mortality: An observational study based on the global burden of disease. *Heliyon*, 9(7).
- Kumar, S., &Mankame, D. P. (2020). Optimization driven deep convolution neural network for brain tumor classification. *Biocybernetics and Biomedical Engineering*, 40(3), 1190-1204.
- Litjens, G., Kooi, T., Bejnordi, B. E., Setio, A. A. A., Ciompi, F., Ghafoorian, M., ... & Sánchez, C. I. (2017). A survey on deep learning in medical image analysis. *Medical image analysis*, 42, 60-88.
- Litjens, G., Sánchez, C. I., Timofeeva, N., Hermsen, M., Nagtegaal, I., Kovacs, I., ... & Van Der Laak, J. (2016). Deep learning as a tool for increased accuracy and efficiency of histopathological diagnosis. *Scientific reports*, 6(1), 26286.
- Machhale, K., Nandpuru, H. B., Kapur, V., &Kosta, L. (2015, May). MRI brain cancer classification using hybrid classifier (SVM-KNN). In *2015 International Conference on Industrial Instrumentation and Control (ICIC)* (pp. 60-65). IEEE.
- Mehnatkesh, H., Jalali, S. M. J., Khosravi, A., &Nahavandi, S. (2023). An intelligent driven deep residual learning framework for brain tumor classification using MRI images. *Expert Systems with Applications*, 213, 119087.
- Özyurt, F., Sert, E., &Avcı, D. (2020). An expert system for brain tumor detection: Fuzzy C-means with super resolution and convolutional neural network with extreme learning machine. *Medical hypotheses*, 134, 109433.
- Parmar, C., Grossmann, P., Bussink, J., &Lambin, P. (2017). Machine learning methods for quantitative radiomic biomarkers. *Machine learning applications for Radiomics*, 5, 125.



- Paul, J. S., Plassard, A. J., Landman, B. A., & Fabbri, D. (2017, March). Deep learning for brain tumor classification. In *Medical Imaging 2017: Biomedical Applications in Molecular, Structural, and Functional Imaging* (Vol. 10137, pp. 253-268). SPIE.
- Ryu, Y. J., Choi, S. H., Park, S. J., Yun, T. J., Kim, J. H., & Sohn, C. H. (2014). Glioma: application of whole-tumor texture analysis of diffusion-weighted imaging for the evaluation of tumor heterogeneity. *PloS one*, 9(9), e108335.
- Saba, T. (2020). Recent advancement in cancer detection using machine learning: Systematic survey of decades, comparisons and challenges. *Journal of Infection and Public Health*, 13(9), 1274-1289.
- Sajjad, M., Khan, S., Muhammad, K., Wu, W., Ullah, A., & Baik, S. W. (2019). Multi-grade brain tumor classification using deep CNN with extensive data augmentation. *Journal of computational science*, 30, 174-182.
- Sasikala, M., & Kumaravel, N. (2008). A wavelet-based optimal texture feature set for classification of brain tumours. *Journal of medical engineering & technology*, 32(3), 198-205.
- Sharif, M. I., Khan, M. A., Alhussein, M., Aurangzeb, K., & Raza, M. (2021). A decision support system for multimodal brain tumor classification using deep learning. *Complex & Intelligent Systems*, 1-14.
- Skogen, K., Schulz, A., Dormagen, J. B., Ganeshan, B., Helseth, E., & Server, A. (2016). Diagnostic performance of texture analysis on MRI in grading cerebral gliomas. *European journal of radiology*, 85(4), 824-829.
- Ting, F. F., Tan, Y. J., & Sim, K. S. (2019). Convolutional neural network improvement for breast cancer classification. *Expert Systems with Applications*, 120, 103-115.
- Verma, R., Zacharaki, E. I., Ou, Y., Cai, H., Chawla, S., Lee, S. K., ... & Davatzikos, C. (2008). Multiparametric tissue characterization of brain neoplasms and their

recurrence using pattern classification of MR images. *Academic radiology*, 15(8), 966-977.

Wulczyn, E., Steiner, D. F., Xu, Z., Sadhwani, A., Wang, H., Flament-Auvigne, I., ...

&Stumpe, M. C. (2020). Deep learning-based survival prediction for multiple cancer types using histopathology images. *PloS one*, 15(6), e0233678.

Zacharaki, E. I., Wang, S., Chawla, S., Soo Yoo, D., Wolf, R., Melhem, E. R., &Davatzikos,

C. (2009). Classification of brain tumor type and grade using MRI texture and shape in a machine learning scheme. *Magnetic Resonance in Medicine: An Official Journal of the International Society for Magnetic Resonance in Medicine*, 62(6), 1609-1618.

Zia, R., Akhtar, P., & Aziz, A. (2018). A new rectangular window based image cropping

method for generalization of brain neoplasm classification systems. *International Journal of Imaging Systems and Technology*, 28(3), 153-162.